Jerez, B., Walla, F., Dios, C. de, Martín-Mateos, P., Acedo, P. (2017). Fully frequency-locked multiheterodyne architecture for remote optical frequency comb rapid detection. *Journal of Lightwave Technology*, 35 (19), pp. 4195-4202

DOI: https://doi.org/10.1109/JLT.2017.2734895

Fully frequency-locked multiheterodyne architecture for remote optical frequency comb rapid detection

Borja Jerez, Frederik Walla, Cristina de Dios, Pedro Martín-Mateos and Pablo Acedo, *Member, IEEE*

***Abstract*—In this paper, a new approach to optical frequency comb (OFC) detection based on a multiheterodyne arrangement is presented. The architecture relies on optical injection locking as a mechanism to induce coherence between an incoming remote OFC and a local oscillator comb with slightly different repetition frequency to retrieve the information encoded in the former. An additional RF locking technique between combs is also implemented, cancelling any frequency drifts and ensuring the temporal stability of the detection scheme while preserving its autonomy from any remote comb. The detection system is validated by recording the coherently averaged transmission spectrum of a fibre Bragg grating sensor imprinted into an electro-optic comb around 1540 nm within 100 µs integration time. While maintaining the range of advantages of dual-comb architectures, such as simultaneous access to manifold spectral points, high resolution and ultra-fast measurement times, the presented system holds promise for being employed as a remote comb detector for different field applications.**

***Index Terms*—Dual Optical Frequency Comb (Dual-comb), Optical Injection Locking (OIL), Optical Interferometry, Remote Comb Detection, Radiofrequency Locking.**

I. Introduction

THE potential of Optical Frequency Combs (OFCs) as coherent, multimode sources is well-known among the scientific community since its inception back in the late 90s [1]. Their capabilities in terms of resolution, broad bandwidth and accuracy have been widely exploited in different fields, such as metrology [2], spectroscopy [3], optical communications [4] or biomedical applications [5], among others. There are a number of techniques in order to retrieve the information associated to each of the teeth of an OFC, namely comb Vernier spectrometers [6], virtually imaged phased arrays (VIPA) spectrometers [7] or Michelson-based Fourier Transform spectrometers [8]. However, in the last years, the dual-comb approach [9] has enjoyed success as a mechanism to fully exploit the extraordinary features of OFCs with additional benefits in terms of acquisition time, resolution and absence of any physical or mechanical limitation of the performance.

The principle of the dual-comb detection approach (also known as dual-comb spectroscopy) relies on the employment of a second OFC (usually denoted as Local Oscillator –LO-) with a slight mismatch in the repetition frequency to heterodyne the primary, or probe comb. The resultant beatnotes between both LO and probe comb yield a new comb in the radiofrequency (RF) domain whose lines are spaced with a frequency value equal to the difference in the repetition frequencies of the OFCs. This way, the discrete structure of the probe OFC is downscaled into the RF domain, where there is a vast number of accessible tools and techniques, while preserving the information encoded in the optical domain.

The virtues of the dual-comb arrangement have led to a number of successful validations using diverse configurations, namely independent free-running lasers [10], [11] and phase-locked lasers [12]–[15], with different laser technologies, such as mode-locked lasers [10]–[14], electro-optically (EO) modulated continuous-wave (CW) lasers [16]–[19] or quantum cascade lasers [20], and in a number of spectral regions (visible [21], near-infrared [12], [13], [15]–[19], [22], mid-infrared [10], [11], [14], [20], THz region [23]). Recently, new techniques, such as Optical Injection Locking (OIL) and Gain-Switching have also been incorporated to the range of existing dual-comb architectures and have been successfully validated [24], [25], extending the capabilities and possibilities associated to these setups. Nevertheless, the complications related to the synchronization of a pair of independent frequency combs usually lead to intricate systems to fully exploit the capabilities of the OFCs concerning precision and resolution [26].

In this paper, a new method for coherent detection of remote OFCs based on a dual-comb architecture is demonstrated. The underlying principle of the presented scheme is twofold: firstly, the selection of one optical line of a remote comb through optical injection to be subsequently used as a carrier to generate a second, local OFC with different mode spacing (also stabilizing the offset frequency); and

Manuscript received XX February 2017, revised XX Month 2017; accepted XX Month 2017. The authors would like to thank the Spanish Ministry of Economy and Competitiveness for supporting the project under the TEC-2014-52147-R (MOSSI). The work by Borja Jerez has been performed in the frame of a FPU Program, #FPU014/06338, granted by the Spanish Ministry of Education, Culture and Sports. The work by Frederik Walla is supported by the European project H2020-MSCA-ITN-2015 (CELTA).

The authors are with the Electronics Technology Department, Universidad Carlos III, Leganés, Madrid, 28911 Spain (e-mails: bjerez@ing.uc3m.es; fwalla@ing.uc3m.es; cdios@ing.uc3m.es; pmmateos@ing.uc3m.es; pag@ing.uc3m.es).

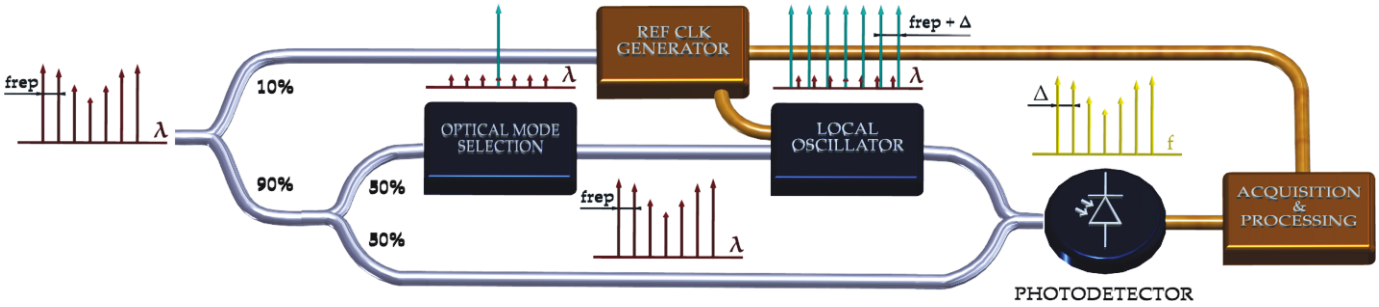

Fig. 1. Basic schematic of the setup. From an entering remote comb, a new local comb with different mode spacing is generated from one line of the former in the detection scheme. The combination of this comb (local oscillator) and the remote comb leads to a new downconverted comb in the RF domain after photodetection. A small part of the remote comb is also employed to generate a reference clock signal to drive (and lock) all the RF generators.

secondly, the generation of a RF signal which allows for the effective lock between both combs by securing the stability of their repetition frequencies without any electrical connection. The final product is a mutually coherent system with capabilities to recover the information carried by a remote comb by means of the dual-comb approach preserving the benefits of EO-generated OFCs in terms of size, higher power per spectral component, lower cost and simplicity of use and control. The system has been validated with the measurement of the deformation of a fibre Bragg grating (FBG) sensor inscribed into a remote comb at 1540 nm.

II. Description Of The Setup

A. General overview

The basic diagram of the proposed setup is shown in Fig. 1, where an incoming remote OFC (with the information of interest encoded in the amplitude and phase of each tooth) enters the detection scheme. A set of optical couplers (with different optical ratios) directs the optical power to fulfil various purposes. First, a small part of the input power (upper branch in Fig. 1) is employed to extract the beatnotes (at f_{REP}) and eventually originate a reference clock signal which will drive all the RF synthesizers and signal generators of the sub-stage where the local comb is generated. The rest of the power is split by means of a 50/50 coupler (lower branches in Fig. 1). While one output remains unaltered (preserving the original remote comb and the information it carries), the other one is used to generate a new comb with a small difference in the frequency spacing $f_{LO}=f_{REP}+\Delta$. For that purpose, one of the lines of the remote comb is filtered through the OIL mechanism to be the seed of a new electro-optically-based OFC.

The combination and detection of these two combs with different repetition rates gives rise not only to a downconversion to the RF domain, but also to a compression of the bandwidth of the comb by a factor of f_{REP}/Δ, leading to a final RF comb with frequency spacing fixed at Δ. From the time-domain point of view, the outcome of this process is two different optical pulse trains with slightly different time delay. When these pulses are merged and heterodyned on a photodetector, a time domain interference pattern pulse train arises which, once Fourier-transformed, brings about the abovementioned RF comb. The final RF signal can, therefore, be acquired and processed by commercial data acquisition boards and software to extract in a parallel way the information engraved in each of the spectral components covered by the remote comb.

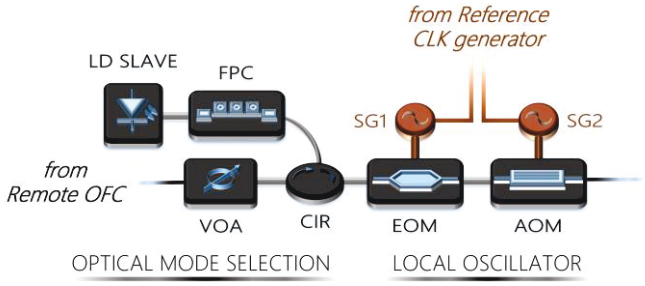

Fig. 2. Detail of the optical mode selection and local oscillator generation sub-stages. LD: Laser diode; VOA: Variable optical attenuator; CIR: Circulator; FPC: Fibre polarization controller; EOM: Electro-optic modulator; AOM: Acousto-optic modulator; SG1/2: Signal generators.

B. Optical mode selection and local oscillator generation

A detailed schematic of the optical mode selection and local oscillator sub-stages is depicted in Fig. 2. The selection of an optical line from the remote comb is based on the OIL mechanism to effectively filter one of the lines while phase-locking to the incoming comb. A further benefit from this process is the stability of the selected line in terms of amplitude, it being adequately isolated from any variation in the amplitude of the remote comb teeth. For that purpose, a CW laser is employed emitting in the wavelength vicinity of the remote comb. A variable optical attenuator and a fibre polarization controller are also incorporated to enable extra control over the injection process. By acting on the current and temperature of the slave laser, its wavelength emission can be tuned into the vicinity of one of the lines of the remote comb, as shown in Fig. 3(a).

Therefore, after adjusting the injection ratio and the polarization state of the injected light, the selected mode of the slave laser becomes the embryo for a new comb (local oscillator comb) (Fig. 3(b)). The light is then electro-optically modulated to create a comb with repetition frequency $f_{LO}=f_{REP}+\Delta$ and also its central frequency is shifted by a value f_{AOM} when going through an acousto-optic modulator (AOM) (Fig. 3(c)). The purpose of this shift is to ensure unequivocal

one-to-one mapping from the optical to the RF domain when heterodyning both remote and local combs, as it was demonstrated in previous works [16]. At this point, it is also important to remark on the fact that this frequency-shift might be dispensable by properly selecting the line to inject [25], but on this occasion it was included so there was not any sort of

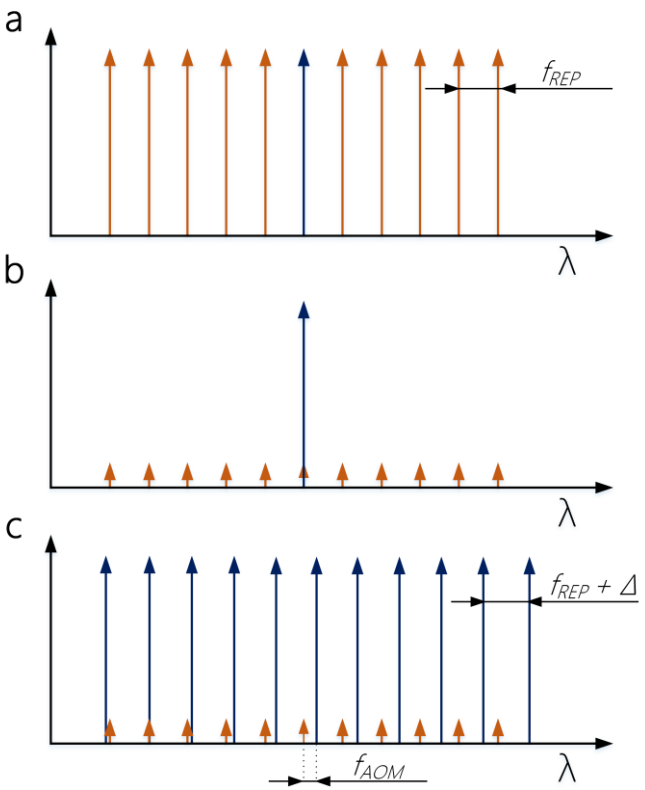

Fig. 3. Local oscillator comb generation process. a) A slave laser is tuned into the proximity of one of the lines of the remote comb with repetition frequency f_{REP}. b) To properly carry out the injection process, strict control over the injection ratio (and polarization state) is kept to select one of the lines of the remote comb as a source to generate a c) new OFC with slightly different spacing ($f_{REP} + \Delta$). An additional frequency shift (f_{AOM}) is introduced to this comb to allow for the unambiguous mapping into the RF domain.

limitation in this sense.

The generation of a local oscillator comb via a filtered line from a remote comb has already proven to be a method for phase tracking two independent combs, valid for superchannel coherent detection [27]. Nevertheless, no technique has been developed to date to recover the information from a remote comb as a whole, and this is the leading motivation of the present work. We demonstrate the detection of the information carried by a remote OFC with the implementation of a multiheterodyne detection stage, supporting the coherent and simultaneous detection of the spectral components of an OFC on a real-time basis. Furthermore, to fully deploy a system with potential remote-comb detection capabilities, it is necessary to implement a RF lock system between combs to guarantee the proper performance of the detection stage while maintaining the independent character of both combs. This will be explained in more detail in the following section.

C. *Reference clock generator*

As a complement to the phase locking between independent combs through OIL, a RF link between combs needs to be achieved. The underlying principle of this method relies on compensating time fluctuations between two independent combs which otherwise may have a negative impact in the form of unwanted drifts in frequency. The importance of the RF locking between independent combs has already been evaluated in the case of free-running, fibre laser-based dual-comb architectures [26].

Since there is no direct RF synchronization between the incoming comb and the LO comb generated in the detection scheme, the RF locking between them stems from the extraction of one of the harmonics from the remote comb at f_{REP} and its further division and signal conditioning to eventually generate a 10 MHz signals which serves as reference for all RF synthesizers. For that purpose, the diagram illustrated in Fig. 4 is implemented.

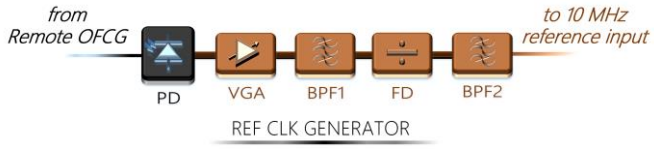

Fig. 4. Detail of the reference clock generator sub-stage. PD: Photodetector; VGA: Variable gain amplifier; BPF1/2: Bandpass filters; FD: Frequency divider.

Although it is not necessary to have information regarding the frequency repetition or amplitude of the teeth of the remote comb, it is necessary to take into account that to properly generate a 10 MHz reference input signal in a real application, both photodetector and frequency divider must provide sufficient versatility for a range of frequencies. Nevertheless, in a proof-of-principle experiment it may be enough to employ a frequency divider with fixed divide ratio and a photodetector fast enough to detect the beatnotes. Similarly, when considering the amplitude of the RF harmonics, one should bear in mind that this value can vary significantly due to a number of factors, such as the remote comb technology, the responsivity of the photodetector or the effect of a target device under test on the remote comb. For these reasons, a mechanism to compensate changes in the RF power of the harmonics should be implemented by means of a variable gain amplifier (VGA) which also provides the frequency divider or the 10 MHz reference input of the generators with the convenient input power. Additional bandpass filters need to be included to get rid of undesired harmonics at multiples of f_{REP} after both photodetection and frequency division.

As a preliminary experiment, the suitability of this mechanism was tested using a frequency mixer. The outputs of two RF generators were employed as inputs for the mixer using the very same frequency without and with external connection between them (i.e., creating a 10 MHz signal from the output of one generator). By using an oscilloscope, a slow oscillation was clearly visible in the unlocked scenario, whereas the oscillation vanished, leading to a constant DC

signal when locking took place, which is clear evidence of the correct RF locking between both synthesizers.

III. Experimental Validation

A. *Implementation of the final system*

The experimental validation of the system was carried out by creating a stage that emulates a remote comb whose spectral information is to be retrieved using the local dual-comb coherent detection scheme (Fig. 5). The final result will therefore be the retrieval of the spectral profile engraved into the remote comb by means of a device under test of interest.

Fig. 5. Overview of the system for experimental validation. A remote comb with spectral information encoded in its teeth is used as input for the detection scheme in order to retrieve the spectral profile generated by a target device under test.

The remote stage encompasses a CW semiconductor laser and an electro-optic modulator to generate a remote OFC which interrogates a device under test. In this case, it consists of a fibre-coupled fibre Bragg grating (FBG) sensor (FiberSensing, Ltd.) with a central wavelength of 1539.98 nm, full width at half maximum (FWHM) of 0.2 nm and a measured sensitivity of 1.11 pm/με. The FBG sensor is attached to a dovetail single-axis linear translation stage (Thorlabs, Inc.) permitting to manually adjust the strain applied to the sensor (and therefore, the transmission spectrum). In principle, the remote comb is arranged so that when no strain is applied, there is no effect on the remote comb lines. Fibre-coupled isolators are also inserted to suppress any reflection between the remote stage and the detection scheme.

The generated OFC with amplitude-encoded information by the FBG is transmitted through 100 m optical fibre and then used as input for the local, detection stage depicted in Fig. 1. An optical coupler is first used to direct 10% of the signal to eventually generate a RF 10 MHz reference. The rest of the power is 50/50 split in what can be regarded as the two arms of an interferometer, as in classic dual-comb architectures. The first half is employed to filter one line of the comb and produce a new one. To that end, a slave CW Discrete Mode laser [28] (EP 1538-5-DM-H19-FM, Eblana Photonics Ltd.) is biased with a current around 115 mA (around 6 dBm). By acting on its temperature, its wavelength emission is roughly tuned around one of the lines of the remote comb (the tuning range of the comb is around 4 nm). A finer adjustment of the injection mechanism is then accomplished with a fibre polarization controller (Thorlabs, Inc.) at the input of the slave laser and also by regulating the power with a variable optical attenuator (AFW Technologies, Inc.). A stable regime with maximized signal-to-noise ratio (SNR) of the RF beatnotes (in the later generated RF comb) was achieved with an injection ratio around -35 dB, as can be seen in Fig. 6 (red lines) for two

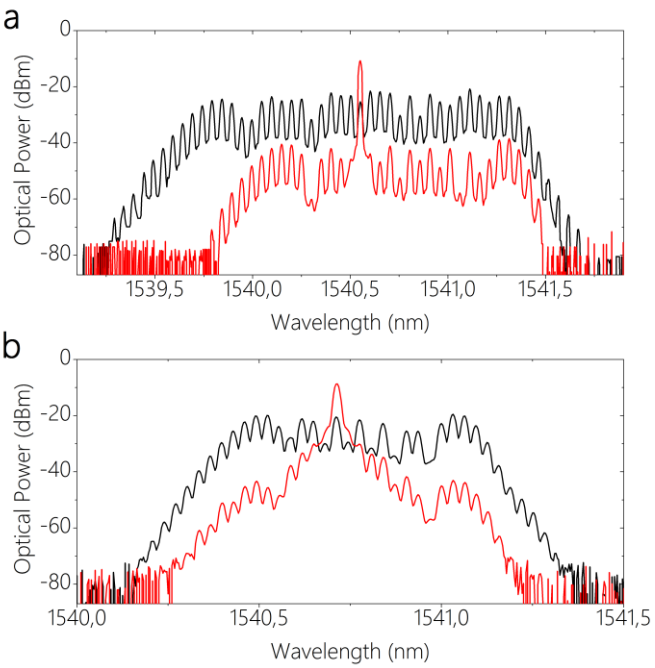

Fig. 6. Illustration of generated OFCs with repetition frequencies of a) 7 GHz and b) 4 GHz. The red lines depict the filtering of a line from the remote comb with an injection ratio around 35 dB, whereas the black lines represent the final mixed comb after combination of the remote and local oscillator combs (with a mismatch in their line spacing of 100 kHz). The screenshots were taken with an optical spectrum analyser with 20 pm resolution.

different repetition frequencies of study (7 GHz and 4 GHz). Both lasers were stabilized in current and temperature with standard laser diode controllers.

The filtered seed line is then used to create the LO comb with an electro-optic phase modulator (PM-5S4-10-PFA-PFA-UV, EOSpace, Inc.) but with a slight difference in the mode spacing Δ of 100 kHz. The RF modulating signal exciting the EOM is amplified up to a power level of 32 dBm. The LO is further frequency-shifted 40 MHz with an AOM (T-M040-0.5C8J-3-F2S, Gooch & Housego, Inc.) driven with a RF power at 24 dBm, to be finally combined with the primary remote comb which travels in the other arm of the interferometer. The polarization state is controlled by means of an additional fibre polarization controller which can alter the polarization state of the remote comb so that it matches with the polarization state of the LO comb. The path mismatch is reduced to maximize the SNR of the RF comb and to decrease the noise floor.

The final (optical) result after merging both remote and local (oscillator) combs is depicted in Fig. 6 (black lines) for the same two repetition frequencies aforementioned. One might infer from this figure that an expansion of the OFC takes place by properly selecting the injection line, but although this is clearly visible in the optical domain, the number of spectral points will always be limited by the narrower comb (and ultimately by the Nyquist criterion). In this sense, it seems apparently crucial that the LO comb had, at least, the same number of lines that the remote comb to correctly extract the information carried by the latter one at once, but considering a general scenario, this limitation may

be overcome with coherent stitching of a number of spectra to recover the full spectral information of the remote comb [13].

The mixture of optical pulses with different time delays corresponding to both LO and remote combs are then heterodyned on an InGaAs photodetector (PDA10CF, Thorlabs, Inc.). The time-domain picture (see Fig. 7) reveals a pulse train caused by a time-domain interference pattern with a separation between pulses equal to the inverse of the difference between the repetition frequencies of the OFCs ($1/\Delta = 10\ \mu s$).

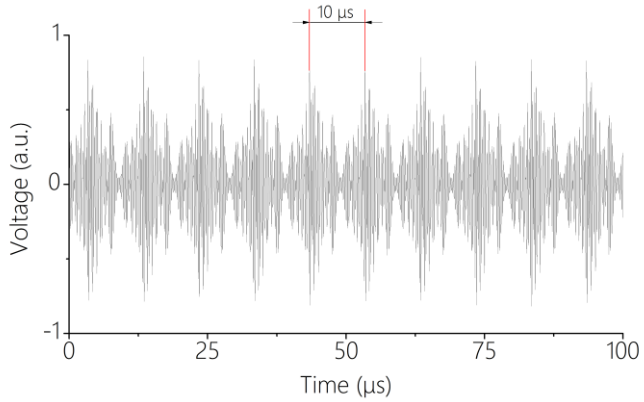

Fig. 7. Time-domain interferogram arisen when the optical pulse trains are photodetected. Each pulse has a centerburst which is caused by the temporal coincidence of two optical pulses in the photodetector. The separation between adjacent pulses is fixed at the inverse of the difference in the line spacing of the OFCs, in this case, 10 µs.

The time-domain signal is then band-pass filtered with standard RF filters to be finally digitized by a 14-bit waveform acquisition board (PDA14, Signatec Inc.). The signal is then synchronously subsampled at 36 MS/s, thus modifying the central frequency to a normalized frequency of 4 MHz at the same time that the repetition rate is kept unmodified at 100 kHz. The Fourier-transformation of the time-domain pulses unveils the RF comb generated, as depicted in Fig. 8. The presence of resolved comb lines is a clear indicator of mutual coherence between both combs. The linewidth of the lines was also assessed with an electrical spectrum analyser, resulting in a linewidth below the minimum resolution bandwidth of the instrument -1 Hz- (sub-Hertz residual linewidth).

B. Analysis of the RF locking

The selected approach to generate a 10 MHz reference signal consists of using an erbium-doped fibre amplifier –EDFA- (Keopsys, Inc.) and a variable optical attenuator (AFW Technologies, Inc.) to have control over the power of the harmonics and adjust it to the input power specifications of the frequency divider and RF generators. A fast photodetector (u2t Photonics, Inc), with 50 GHz bandwidth was employed, as well as fixed ratio (N) frequency dividers (being $N=f_{REP}/10MHz$) and standard band-pass filters (Minicircuits, Inc.). Alternatively, a broadband RF amplifier (with fixed or variable gain) can also be employed to alleviate the requirements of either the EDFA or the photodetector.

The impact of the RF reference locking signal on the generated RF comb was then evaluated. Fig. 9 shows a first

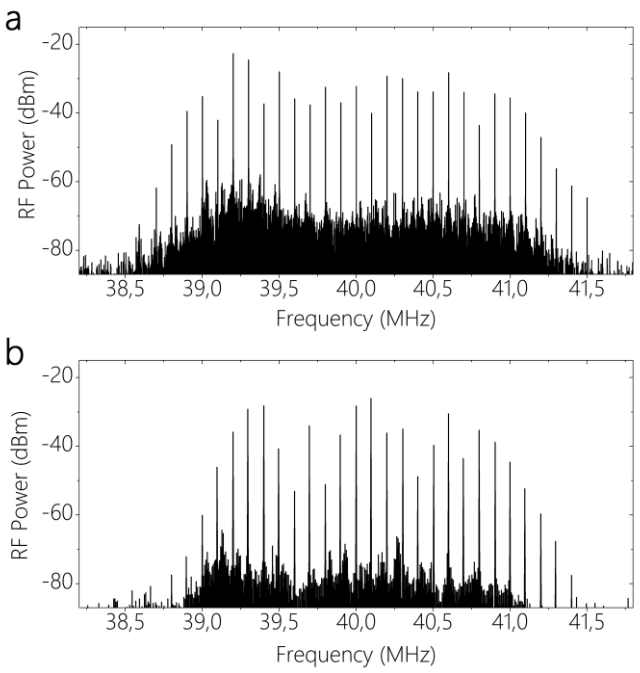

Fig. 8. Illustration of the RF combs generated after Fourier-transforming the signal impinged on the photodetector. The central line corresponds to the frequency-shift induced by the AOM (40 MHz) and the line spacing to the mismatch between repetition frequencies of the combs (100 kHz). Two different cases for two values of OFC repetition frequencies: a) 7 GHz; b) 4 GHz. The discrepancies in bandwidth and number of lines are mainly due to the response of the two different amplifiers used to drive the EOMs for each of these frequencies.

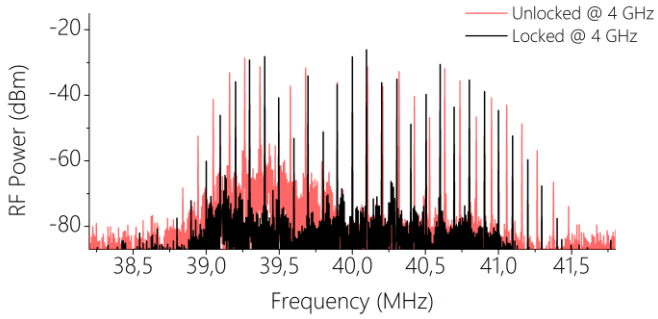

Fig. 9. Comparison between two RF combs generated from OFCs with 4 GHz repetition frequency (and 100 kHz separation) without (red line) and with (black line) RF locking between independent combs. An increasing frequency drift is observed in the unlocked scenario as a direct translation from the optical domain.

consequence of keeping the combs RF-unlocked. Together with an increase of the noise floor, a frequency drift appears between lines which increases as the lines are farther from the centre of the RF comb, which is a direct consequence of an optical drift between both remote and LO combs. The quantified frequency deviation is 56 kHz/MHz, which translated into the optical domain corresponds to 7.07 GHz/nm. Additionally, an analysis of the time stability of the lines of the RF comb was realized. To this end, the temporal evolution of the 5th line on the right side of the central line (i.e., the line at 40.5 MHz in the locked case, and at 40.528 MHz –due to the drift- in the unlocked case) was recorded during a 20-minute experiment with an electrical spectrum

analyser (see Fig. 11). The results reveal a time-varying offset of the line when no locking between synthesizers takes place with respect to its central frequency (reaching up to hundreds of hertzs). On the contrary, when the locking takes effect, no sign of frequency mismatch is noticed during the time of the experiment, and the evaluated line preserves its initial and expected frequency value.

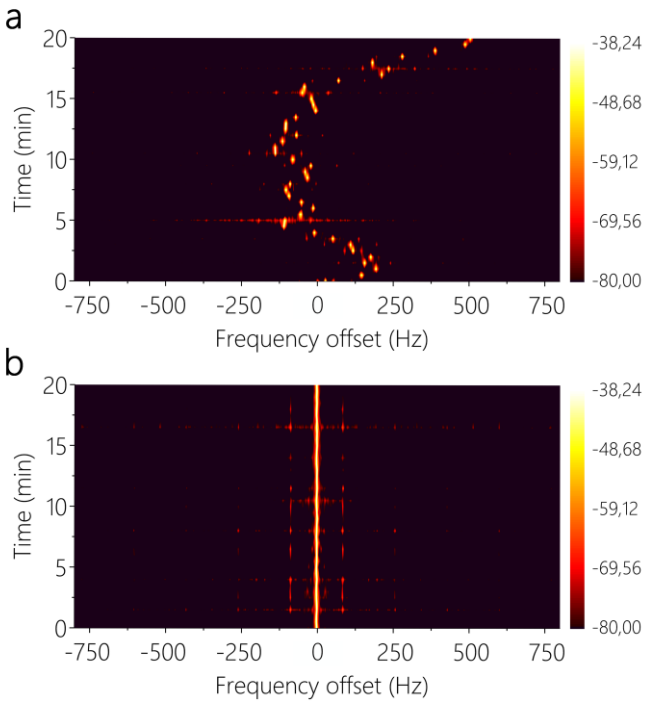

Fig. 11. Temporal evolution of the frequency associated to the 5th line (right side) of the RF comb (at 40.528 MHz and 40.5 MHz under unlocked and locked conditions, respectively). a) Unlocked case. Continuous drifts from the initial frequency are observed along the experiment, lacking any time stability. b) Locked case. No frequency deviation is observed, remaining the theoretical value unchanged. Two measurements each minute were taken during 20 minutes with an electrical spectrum analyser. Resolution bandwidth: 2 Hz.

C. Measurement of a fibre Bragg grating sensor

Finally, the complete system was validated with the measurement of the transmission spectrum of the FBG sensor to detect the effect caused by a deformation on it. Since the FBG sensor is conveniently attached to the linear translation stage, it is enough to slightly move the stage along its axis to exert strain. The results are illustrated in Fig. 10, where the ratio between a reference (no strain) and an actual measurement (with strain –around 490 με-) is depicted for two different comb repetition frequencies (7 GHz and 4 GHz). It is important to note that, in any case, both measurements (reference for normalization, and effective measurement) originate from the remote comb. The dots show the profile after an average of 10 measurements over an integration time of 100 μs for a repetition frequency of 7 GHz (Fig. 10 (a)). The same integration time, but an average of 15 measurements was performed for a line spacing of 4 GHz (Fig. 10 (b)). In both cases, a Voigt fit is performed, showing agreement with the expected value of FWHM. The residuals between the

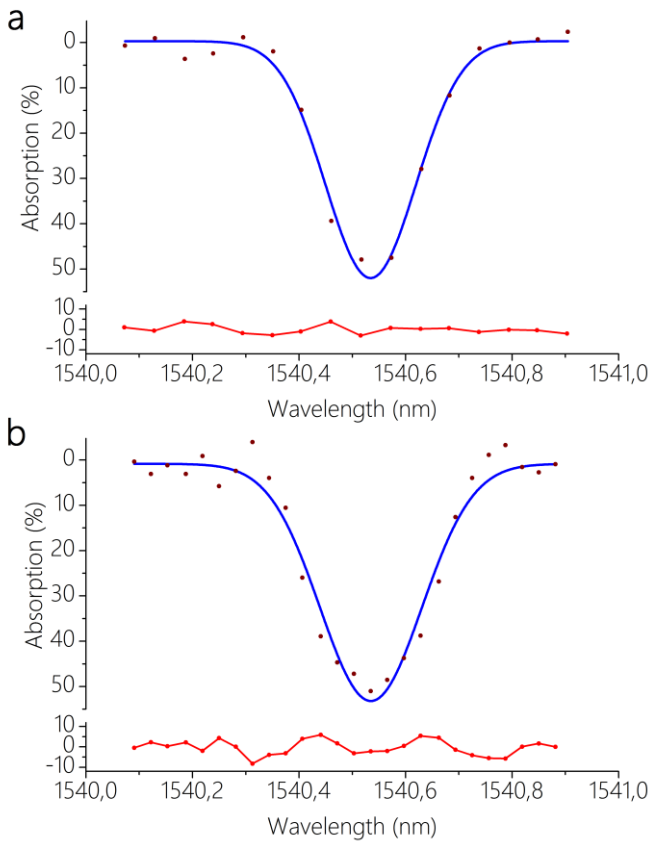

Fig. 10. Transmission spectrum (dots) of the FBG sensors when interrogated with combs with repetition frequency of a) 7 GHz and b) 4 GHz. The applied strain is roughly 490 με, which leads to a wavelength shift in the transmission spectrum of 0.54 nm. The blue line shows a Voigt fit in both cases, representing a FWHM of a) 0.20 nm and b) 0.23 nm. The residuals (red lines) reveal a standard deviation of a) 2.11% and b) 3.63%. The integration time in each case is set at 100 μs. The number of averages is 10 and 15, respectively.

experimental data and the fit reveal a standard deviation of 2.11% and 3.63% for 7 GHz and 4 GHz, respectively. The average SNR of the lines of the comb (at 7 GHz and 1 ms integration time) is 5845, but after normalizing this figure accordingly to the number of spectral points and for a standard integration time of 1 s, a value of 5.5×10^6 is obtained for the figure of merit defined as SNR × M at 1 s [29] (where M stands for the number of spectral points, in this case 30).

As a final remark, it has to be said that the maximum resolution of the system will be ultimately limited by the injection locking mechanism. It has been reported in previous work that the existence of neighbouring lines in an OFC may provoke undesired perturbations when a *guard* or free-spectral region between two lines is not taken into consideration when injecting [27]. In the presented system, this is translated into disturbances in the RF comb, which may lead to increased noise due to locking crosstalk or the eventual loss of spectral points. We found that, with our instruments, our resolution limit lies around 4 GHz (which might explain the discrepancies between the profiles in Fig. 10). However, this resolution limit might be enhanced with the use of ultra-low noise laser controllers, with the inclusion of feedback loops from the photodetector to the laser controller [30] or even

avoided by accomplishing frequency sweeps and interleaving spectra [20].

IV. Conclusions

We have introduced a novel system for OFC detection which allows for the retrieval of the information imprinted into a remote comb as a whole by means of a local multiheterodyne detection scheme. The system exploits the benefits of the OIL mechanism to generate a phase-locked local OFC with stable offset frequency and different frequency spacing from a filtered line of a sensing, remote comb, yielding mutual coherence between both combs and thus fully resolved RF spectrum with sub-Hz linewidth. A straightforward method to lock and synchronize all RF synthesizers (and hence, both combs and their repetition frequencies) also endows the system with time stability, allowing for the recording of free-distortion spectra and coherent averaging.

The architecture is validated with the detection of an electro-optic OFC and the measurement of deformation of a FBG sensor. The very high mutual coherence of the system permits the recovery of the FBG transmission spectrum by averaging with an integration time of 100 μs. The system preserves all the virtues associated to classic dual-comb spectroscopy in terms of simultaneous and accurate access to multiple spectral points within a short period of time. Although the resolution is eventually defined by the OIL mechanism, future work on this line may expand the capabilities of the system to field detection and study of low-pressure target gases with narrower linewidths, taking full advantage of the easy-to-handle and field deployable idiosyncrasy of compact, inexpensive EOM-based detection architectures.

References

[1] T. W. Hänsch, "Nobel Lecture: Passion for precision," *Rev. Mod. Phys.*, vol. 78, no. 4, pp. 1297–1309, 2006.

[2] T. Udem, R. Holzwarth, and T. W. Hänsch, "Optical frequency metrology," *Nature*, vol. 416, no. 6877, pp. 233–237, 2002.

[3] T. Udem, "Spectroscopy: frequency comb benefits," *Nat. Photonics*, vol. 3, no. 2, pp. 82–84, 2009.

[4] P. J. Delfyett, S. Gee, C. Myoung-Taek, H. Izadpanah, L. Wangkuen, S. Ozharar, F. Quinlan, and T. Yilmaz, "Optical frequency combs from semiconductor lasers and applications in ultrawideband signal processing and communications," *J. Light. Technol.*, vol. 24, no. 7, pp. 2701–2719, 2006.

[5] T. Ideguchi, S. Holzner, B. Bernhardt, G. Guelachvili, N. Picqué, and T. W. Hänsch, "Coherent Raman spectro-imaging with laser frequency combs," *Nature*, vol. 502, no. 7471, pp. 355–358, 2013.

[6] C. Gohle, B. Stein, A. Schliesser, T. Udem, and T. W. Hänsch, "Frequency comb vernier spectroscopy for broadband, high-resolution, high-sensitivity absorption and dispersion spectra," *Phys. Rev. Lett.*, vol. 99, no. 26, 2007.

[7] S. A. Diddams, L. Hollberg, and V. Mbele, "Molecular fingerprinting with the resolved modes of a femtosecond laser frequency comb.," *Nature*, vol. 445, no. 7128, pp. 627–630, 2007.

[8] P. R. Griffiths and J. A. De Haseth, *Fourier Transform Infrared Spectrometry*, 2nd ed. John Wiley & Sons, 2007.

[9] S. Schiller, "Spectrometry with frequency combs," *Opt. Lett.*, vol. 27, no. 9, pp. 766–768, 2002.

[10] F. Keilmann, C. Gohle, and R. Holzwarth, "Time-domain mid-infrared frequency-comb spectrometer," *Opt. Lett.*, vol. 29, no. 13, pp. 1542–1544, 2004.

[11] A. Schliesser, M. Brehm, F. Keilmann, and D. van der Weide, "Frequency-comb infrared spectrometer for rapid, remote chemical sensing," *Opt. Express*, vol. 13, no. 22, pp. 9029–9038, 2005.

[12] I. Coddington, W. C. Swann, and N. R. Newbury, "Coherent multiheterodyne spectroscopy using stabilized optical frequency combs," *Phys. Rev. Lett.*, vol. 100, no. 1, p. 13902, 2008.

[13] I. Coddington, W. C. Swann, and N. R. Newbury, "Coherent dual-comb spectroscopy at high signal-to-noise ratio," *Phys. Rev. A*, vol. 82, no. 4, p. 43817, 2010.

[14] E. Baumann, F. R. Giorgetta, W. C. Swann, A. M. Zolot, I. Coddington, and N. R. Newbury, "Spectroscopy of the methane ν3 band with an accurate midinfrared coherent dual-comb spectrometer," *Phys. Rev. A*, vol. 84, no. 6, p. 62513, 2011.

[15] A. M. Zolot, F. R. Giorgetta, E. Baumann, J. W. Nicholson, W. C. Swann, I. Coddington, and N. R. Newbury, "Direct-comb molecular spectroscopy with accurate, resolved comb teeth over 43 THz," *Opt. Lett.*, vol. 37, no. 4, pp. 638–640, Feb. 2012.

[16] D. A. Long, A. J. Fleisher, K. O. Douglass, S. E. Maxwell, K. Bielska, J. T. Hodges, and D. F. Plusquellic, "Multiheterodyne spectroscopy with optical frequency combs generated from a continuous-wave laser," *Opt. Lett.*, vol. 39, no. 9, pp. 2688–2690, 2014.

[17] P. Martin-Mateos, M. Ruiz-Llata, J. Posada-Roman, and P. Acedo, "Dual-comb architecture for fast spectroscopic measurements and spectral characterization," *IEEE Photonics Technol. Lett.*, vol. 27, no. 12, pp. 1309–1312, 2015.

[18] P. Martín-Mateos, B. Jerez, and P. Acedo, "Dual electro-optic optical frequency combs for multiheterodyne molecular dispersion spectroscopy," *Opt. Express*, vol. 23, no. 16, pp. 21149–58, 2015.

[19] G. Millot, S. Pitois, M. Yan, T. Hovhannisyan, A. Bendahmane, T. W. Hänsch, and N. Picqué, "Frequency-agile dual-comb spectroscopy," *Nat. Photonics*, vol. 10, no. May, pp. 27–30, 2016.

[20] G. Villares, A. Hugi, S. Blaser, and J. Faist, "Dual-comb spectroscopy based on quantum-cascade-laser frequency combs," *Nat. Commun.*, vol. 5, p. 5192, 2014.

[21] T. Ideguchi, A. Poisson, G. Guelachvili, T. W. Hänsch, and N. Picqué, "Adaptive dual-comb spectroscopy in the green region," *Opt. Lett.*, vol. 37, no. 23, pp. 4847–4849, 2012.

[22] B. Bernhardt, A. Ozawa, P. Jacquet, M. Jacquey, Y. Kobayashi, T. Udem, R. Holzwarth, G. Guelachvili, T. W. Hänsch, and N. Picqué, "Cavity-enhanced dual-comb spectroscopy," *Nat. Photonics*, vol. 4, no. 1, pp. 55–57, 2009.

[23] T. Yasui, M. Nose, A. Ihara, K. Kawamoto, S. Yokoyama, H. Inaba, K. Minoshima, and T. Araki, "Fiber-based, hybrid terahertz spectrometer using dual fiber combs," *Opt. Lett.*, vol. 35, no. 10, pp. 1689–1691, 2010.

[24] B. Jerez, P. Martín-Mateos, E. Prior, C. de Dios, and P. Acedo, "Dual optical frequency comb architecture with capabilities from visible to mid-infrared," *Opt. Express*, vol. 24, no. 13, pp. 14986–94, 2016.

[25] B. Jerez, P. Martín-Mateos, E. Prior, C. De Dios, and P. Acedo, "Gain-switching injection-locked dual optical frequency combs: characterization and optimization," *Opt. Lett.*, vol. 41, no. 18, pp. 4293–4296, 2016.

[26] T. Ideguchi, A. Poisson, G. Guelachvili, N. Picqué, and T. W. Hänsch, "Adaptive real-time dual-comb spectroscopy," *Nat. Commun.*, vol. 5, p. 3375, 2014.

[27] A. C. Bordonalli, M. J. Fice, and A. J. Seeds, "Optical injection locking to optical frequency combs for superchannel coherent detection.," *Opt. Express*, vol. 23, no. 2, pp. 1547–1557, Jan. 2015.

[28] C. Herbert, D. Jones, A. Kaszubowska-Anandarajah, B. Kelly, M. Rensing, J. O'Carroll, R. Phelan, P. Anandarajah, P. Perry, L. P. Barry, and J. O'Gorman, "Discrete mode lasers for communication applications," *IET Optoelectron.*, vol. 3, no. 1, pp. 1–17, Feb. 2009.

[29] I. Coddington, N. Newbury, and W. Swann, "Dual-comb spectroscopy," *Optica*, vol. 3, no. 4, pp. 414–426, 2016.

[30] M. J. Fice, A. Chiuchiarelli, E. Ciaramella, and A. J. Seeds, "Homodyne coherent optical receiver using an optical injection phase-lock loop," *J. Light. Technol.*, vol. 29, no. 8, pp. 1152–1164, 2011.

Borja Jerez received the B.Sc. degree in industrial electronics and automation in 2013 and the M.Sc. degree in industrial engineering in 2015 from the Universidad Carlos III Madrid, Leganés, Spain, both with honors. Since October 2015, he has been working toward the Ph.D. degree in electrical engineering, electronics and automation at Universidad Carlos III.

Since 2013, he has been working with the Optoelectronics and Laser Technology Group in Universidad Carlos III Madrid. His research interests involve the analysis and design of advanced multimode optical sources (optical frequency comb generators) and the development and implementation of new architectures in various regions of the electromagnetic spectrum for measurement and detection of volatile organic compounds and fiber optic sensors for spectroscopy and industrial applications.

Frederik Walla received the B.S. degree in physics from Technische Universität Darmstadt, Darmstadt, Germany, in 2012 and the M.S. degree in physics with distinction from Goethe University Frankfurt, Frankfurt, Germany, in 2016. He is currently pursuing the Ph.D. degree in electrical engineering, electronics and automation at Universidad Carlos III de Madrid, Madrid, Spain.

His current research is conducted within the framework of CELTA ITN, aiming towards the convergence of electronics and photonics technologies for enabling terahertz applications. His research interest includes the development of multimode laser sources (optical frequency combs) for their application in photonic signal synthesis, terahertz generation and detection, spectroscopy and near-field optical microscopy

Cristina de Dios received the Doctorate degree in 2010 for her work in ultrafast pulsed diode lasers and nonlinear pulse compression at the Universidad Carlos III de Madrid, Madrid, Spain.

Currently, she is an associate professor at the Electronics Technology Department and a member of the Optoelectronics and Laser Technology Group in this same university. Her research interests are optical frequency comb generation techniques, pulsed semiconductor laser sources, nonlinear optical phenomena and sub-terahertz and millimeter wave photonic signal synthesis and detection.

Pedro Martín-Mateos received his MSc in Telecommunication Engineering, his MRes in Advanced Electronics Systems and a Ph.D. degree in Electrical Engineering, Electronics and Automation from Universidad Carlos III de Madrid (Spain) in 2010, 2013 and 2015 respectively. In 2015 he was appointed as Assistant Professor by Universidad Carlos III de Madrid.

From 2011, he has been involved in research activities for the development of new techniques and architectures for fluorescence spectroscopy, Diffuse Reflectance spectroscopy, Molecular Dispersion spectroscopy and Optical Frequency Comb spectroscopy for biomedical and environmental applications.

Pablo Acedo received his Doctorate (with honors) from the Universidad Carlos III de Madrid in 2000 for his work on heterodyne two color laser interferometry for fusion plasma diagnostics. His doctoral work included the development of the first two color laser system based on Mid-IR sources for a Stellarator Fusion Device (Stellarator TJ-II) and the first two-color Nd:YAG system for a Fusion Device (Tokamak C-Mod), the latter during several doctoral visits to MIT during the years 1996-1999.

In 2002 he was appointed Assistant Professor by Universidad Carlos III de Madrid where he continued with the development of scientific instrumentation systems for fusion plasma diagnostics and biomedical applications, leading national projects and contracts on these fields. During the last years, he has been very active in the development of advanced spectroscopy techniques, mainly based on multiheterodyne architectures using Dual-Optical Frequency Combs, with applications in fields like gas spectroscopy (new dispersion spectroscopy techniques), environmental applications (with important impact in the media), and, especially, in biomedical applications (tissue engineering, metabolomics)

Prof. Acedo has published more than 90 contributions in journals and international conferences, including invited conferences and seminars. He has been part in more than 30 projects/contracts with companies, being the head researcher in 12 of them. He is a named inventor in 2 patents and has supervised 3 Ph.D. theses.